

## Cutinase-Catalyzed Hydrolysis of Poly(ethylene terephthalate)

Åsa M. Ronkvist, Wenchun Xie, Wenhua Lu, and Richard A. Gross\*

NSF I/URC for Biocatalysis and Bioprocessing of Macromolecules, Department of Chemical and Biological Sciences, Polytechnic University, Six Metrotech Center, Brooklyn, New York 11201

Received March 11, 2009; Revised Manuscript Received May 23, 2009

**ABSTRACT:** A detailed study and comparison was made on the catalytic activities of cutinases from *Humilica insolens* (HiC), *Pseudomonas mendocina* (PmC), and *Fusarium solani* (FsC) using low-crystallinity (*lc*) and biaxially oriented (*bo*) poly(ethylene terephthalate) (PET) films as model substrates. Cutinase activity for PET hydrolysis was assayed using a pH-stat to measure NaOH consumption versus time, where initial activity was expressed as units of micromoles of NaOH added per hour and per milliliter of reaction volume. HiC was found to have good thermostability with maximum initial activity from 70 to 80 °C, whereas PmC and FsC performed best at 50 °C. Assays by pH-stat showed that the cutinases had about 10-fold higher activity for the *lc*PET (7% crystallinity) than for the *bo*PET (35% crystallinity). Under optimal reaction conditions, initial activities of cutinases were successfully fit by a heterogeneous kinetic model. The hydrolysis rate constant  $k_2$  was 7-fold higher for HiC at 70 °C (0.62  $\mu\text{mol}/\text{cm}^2/\text{h}$ ) relative to PmC and FsC at 50 and 40 °C, respectively. With respect to PET affinity, PmC had the highest affinity, while FsC had the lowest value. In a 96 h degradation study using *lc*PET films, incubation with PmC and FsC both resulted in a 5% film weight loss at 50 and 40 °C, respectively. In contrast, HiC-catalyzed *lc*PET film hydrolysis at 70 °C resulted in a  $97 \pm 3\%$  weight loss in 96 h, corresponding to a loss in film thickness of 30  $\mu\text{m}$  per day. As degradation of *lc*PET progressed, crystallinity of the remaining film increased to 27% due to preferential degradation of amorphous regions. Furthermore, for all three cutinases, analysis of aqueous soluble degradation products showed that they consist exclusively of terephthalic acid and ethylene glycol.

### Introduction

Poly(ethylene terephthalate) (PET) is the highest-volume polyester produced and is used in numerous applications such as films, fibers, and packaging. It is the most commonly used synthetic fiber (25 million tonnes produced annually worldwide) and is forecasted to account for almost 50% of all fiber materials in 2008.<sup>1</sup> A disadvantage of PET is its hydrophobic nature, resulting in poorly wettable surfaces. As a consequence, difficulties with PET fibers are encountered when applying finishing compounds and coloring agents. Furthermore, PET fibers with hydrophobic surfaces build up electrostatic charges and are prone to bacterial adhesions. Therefore, methods for PET surface modification are important to those who manufacture PET for the textile, biomedical, microelectronic, and packaging industries. Common means for surface hydrophilization range from chemical (e.g., alkali, etching) to plasma treatments.<sup>2</sup> An interesting alternative is the use of enzymes for polyester surface modification.<sup>3–9</sup> Advantages of enzymatic methods include their action under mild conditions with low energy input without the need for expensive machinery. Furthermore, enzyme-catalyzed hydrolysis is restricted to material surfaces due to the large size and incompatibility of enzymes with polymeric substrates. Hence, enzymatic hydrolysis has the potential to provide large changes in surface functionality while not affecting bulk properties.<sup>2,7</sup> Thus far, PET hydrolyzing activity has been reported for members of the cutinase,<sup>3,5–8,10</sup> lipase,<sup>3,7,10,11</sup> and esterase<sup>3,4</sup> families. Relative to lipases and esterases, cutinases have shown the greatest promise for PET hydrolysis.<sup>3,7,10,11</sup> It was demonstrated that the treatment of PET with cutinases from *Pseudomonas mendocina*,<sup>5</sup> *Fusarium solani*,<sup>3</sup> and *Thermobifida*

*fusca*<sup>3</sup> result in enhanced surface hydrophilicity and increased cationic dye binding. Araújo et al.<sup>8</sup> genetically modified and enlarged the active site of *F. solani pisi* cutinase in order to improve the fit between its active site and PET chains. Indeed, they reported that the new variants showed improvement in activity 5-fold relative to the wild-type enzyme for PET hydrolysis.<sup>8</sup>

Apart from surface modification, enzymes are also a potential tool for PET degradation.<sup>10–12</sup> The predicted lifetime of PET ranges from 25 to 50 years.<sup>13</sup> PET products are the premier recyclable plastic with a recycle value only second to aluminum. However, for certain PET product forms, such as thin films, textiles, or composite structures, recycling of PET is uneconomical. In these cases, degrading PET would provide an alternative strategy to recover value.<sup>13</sup> Until recently, PET was regarded as nondegradable with excellent hydrolytic stability.<sup>10–13</sup> PET can be chemically hydrolyzed, but harsh chemical conditions such as using sulfuric acid at 150 °C are required.<sup>12</sup> Attempts to improve its susceptibility to hydrolysis has included increasing the content of aliphatic repeat units along the chains.<sup>10,12,13</sup> The potential of using enzymatic catalysis for PET recycling was recently demonstrated by Müller et al.<sup>11</sup> who treated commercial PET of low-crystallinity (9%) from soft drink bottles with a cutinase from *T. fusca* at 55 °C. They reported achieving a weight loss of 50% after 3 weeks and a decrease in thickness per week of 17  $\mu\text{m}$ .

Previous studies<sup>5,7,11</sup> reported that high crystallinity negatively affects cutinase activity for PET hydrolysis. Indeed, it is well-known that polymer chain mobility in the amorphous<sup>14</sup> and crystalline<sup>15</sup> regions plays an important role in regulating the rate of enzyme-catalyzed polyester hydrolysis.<sup>16,17</sup> Furthermore, enzymatic hydrolysis of polyesters occurs more rapidly by conducting biotransformations at temperatures closely approaching the glass transition temperature of amorphous polyesters or the melting point of semicrystalline polyesters.<sup>18–21</sup>

\*To whom correspondence should be addressed. E-mail: rgross@poly.edu.

Herein, we report a detailed study and comparison of the catalytic activities of cutinase from three different organisms, using low-crystallinity (7%) PET films (*lc*PET) as substrates. The affect of crystallinity on cutinase-catalyzed degradation was determined using biaxially oriented PET films (*bo*PET) with 35% crystallinity. Three different cutinases were included in this study, specifically those from *Humicola insolens* (HiC), *Pseudomonas mendocina* (PmC), and *Fusarium solani* (FsC). These cutinases were first purified (>95%) and are quantified in nanomoles per milliliter. This is in contrast to previous publications on enzyme-catalyzed PET degradation where enzyme quantification relied on activity units.<sup>4,7,8,22</sup> Studies were conducted to elucidate effects of pH and temperature on initial rates of cutinase-catalyzed *lc*PET degradation. Kinetics of cutinase-catalyzed *lc*PET hydrolysis were performed, and the results were fit to kinetic models. The only other literature report on PET-like substrates where kinetic data were reported was by Figueroa et al.<sup>23</sup> However, they used cutinase from Novozyme with unknown origin, and the substrate was cyclo-tris-ethylene terephthalate. To determine kinetic parameters, rates of cutinase-catalyzed PET hydrolysis were measured with a pH-stat, which directly monitors released acid during ester cleavage. Cutinase-catalyzed PET hydrolysis was also studied by measuring PET film weight loss. Results obtained from film weight loss were successfully correlated to determinations of film degradation by high-performance liquid chromatography (HPLC) analysis of formed degradation products. Furthermore, results of weight loss allowed comparisons to extents of enzyme-catalyzed PET degradation reported elsewhere.<sup>3,5,7</sup>

## Materials and Methods

**Materials.** HiC and PmC were kind gifts from Novozymes (Bagsvaerd, Denmark) and Genencor (Danisco US Inc., Genencor Division, Palo Alto, CA), respectively. Wild-type FsC cloned into *Pichia pastoris* was purchased from DNA 2.0 (Menlo Park, CA). Methods for fermentative synthesis and purification of FsC are given in the companion paper.<sup>24</sup> Low-crystallinity PET films (*lc*PET, product number 029-198-54) and biaxially oriented PET films (*bo*PTE, product number 543-716-95), both with a thickness of 250  $\mu\text{m}$ , were purchased from Goodfellow Co. Terephthalic acid (TPA) and bis(2-hydroxyethyl) terephthalate (BHET), used as standard samples for HPLC analysis, were purchased from Fluka and Sigma, respectively. Mono(2-hydroxyl ethyl) terephthalate (MHET), also used for HPLC analysis, was obtained as a mixture with water by hydrolyzing BHET with KOH at 75 °C for 60 min. All other chemicals were purchased from Sigma-Aldrich Co in the highest available purity and were used without further purification.

**Cutinase-Catalyzed PET Hydrolysis Monitored by pH-stat.** Cutinase activity for PET hydrolysis was assayed using a pH-stat apparatus (Titrand 842, Metrohm) equipped with Tiamo 1.1 software according to the method given in the companion paper.<sup>24</sup> In summary, PET films with dimensions 5  $\times$  5 mm<sup>2</sup> were used in order to achieve good stirring, and the PET concentration was expressed as square centimeters per milliliter. Initial PET hydrolysis rates were expressed as units of micromoles of added NaOH per hour and milliliter of reaction volume. Studies of enzyme activity on PET in pH-stat experiments were performed over temperatures from 30 to 90 °C, pH values of 6.5–9.5, cutinase concentrations of 0–12 nmol/mL, and PET concentrations of 0–40 cm<sup>2</sup>/mL. All reactions were performed in duplicate. Control samples (without enzyme) were run for each parameter in order to determine background chemical hydrolysis, which was subtracted from the total hydrolysis to measure enzyme-catalyzed PET hydrolysis.

**Degradation Studies.** A PET film (15  $\times$  15 mm<sup>2</sup>) with a thickness of 250  $\mu\text{m}$  was placed in a vial containing 3 mL of a

Tris-HCl buffer (pH 8.0) with 10% glycerol and 10  $\mu\text{M}$  of one of the cutinases. Studies on the effect of the Tris buffer concentration (0–1 M) and time course studies were performed by placing vials in a rotary shaker–incubator at 100 rpm, from 0 to 96 h, at optimal temperature values determined from pH-stat experiments (see above). At sampling times, three replicate vials for each cutinase were removed from the shaker–incubator; films were washed extensively with distilled water, dried in vacuo (30 mmHg) for 24 h at 40 °C, and then weighed. Weight loss was calculated by subtracting the final weight from the initial weight. Control samples (without enzyme) were also carried out in triplicate in order to account for potential contribution to weight loss by chemical hydrolysis. Final weight loss values due to cutinase-catalyzed hydrolysis were calculated by subtracting background weight loss attributed to chemical hydrolysis.

**Scanning Electron Microscopy (SEM) Imaging.** The morphology of PET films before and after enzyme exposure was examined by SEM on a Hitachi S-570 model at an accelerating voltage of 20 kV. Samples were coated with gold in an argon field using a Pelco 91000 sputter coater for 140 s at 18 mA. Digitized images were brought into Epax genesis software for assembly.

**Differential Scanning Calorimetry (DSC).** PET films from degradation studies and original low-crystallinity and biaxially oriented PET films (as received) were analyzed by DSC using a TA Instruments Q100 DSC, equipped with an LNCS low-temperature accessory. DSC scans were run in the temperature range from 0 to 300 °C under a dry nitrogen atmosphere. All runs were carried out at a heating rate and cooling rate of 10 °C/min, and PET sample weights were about 10  $\pm$  2 mg.

To establish the degree of crystallinity, the heat of fusion,  $\Delta H_m$ , and cold crystallization,  $\Delta H_c$ , were determined by integrating areas ( $\text{J g}^{-1}$ ) under peaks. The percent crystallinity was calculated using the following equation:

$$\text{crystallinity (\%)} = \frac{|\Delta H_m| - |\Delta H_c|}{\Delta H_m^\circ} \times 100 \quad (1)$$

where  $\Delta H_m^\circ$  is the heat of fusion for a 100% crystalline polymer, which is estimated to be 140.1  $\text{J g}^{-1}$ .<sup>7,25</sup>

**Reversed-Phase HPLC.** The incubation media collected from degradation studies were analyzed by HPLC using a similar method to that developed by Vertommen et al.<sup>7</sup> The HPLC system consisted of a Waters 2795 separation module and a Waters 2996 photo diode array detector (Milford, MA). The separation was carried out on a Phenomenex Synergi Hydro-RP column (4  $\mu\text{m}$ , 250 mm  $\times$  4.6 mm i.d.) run under isocratic conditions. The mobile phase was composed of 70% water, 20% acetonitrile, and 10% formic acid solution (v/v), and the flow rate was 1 mL/min. Standard solutions were mixtures of TPA and BHET at concentrations of 0.5, 1, 5, 10, and 25  $\mu\text{g/mL}$ . Calibration curves of TPA and BHET were constructed by plotting the peak area of TPA and BHET at a wavelength of 244 nm versus concentrations of standard solutions.

## Results and Discussion

**DSC Studies of *lc*- and *bo*PET.** Low-crystallinity and biaxially oriented PET films (*lc*PET and *bo*PET, respectively) were characterized by DSC. The first heating scan of *lc*PET, Figure 1a, showed a clear glass transition temperature ( $T_g$ ) at 75 °C, a cold crystallization peak at 142 °C, and a melting temperature ( $T_m$ ) at 247 °C. The cold crystallization peak originates from crystallization of the amorphous regions.<sup>26</sup> In contrast, the thermogram of *bo*PET (Figure 1b) displayed at 253 °C, but transitions associated with crystallization and  $T_g$  were not seen. The degree of crystallinity values for *lc*PET and *bo*PET, calculated using eq 1 above, are 7.0  $\pm$  0.5% and 35.0  $\pm$  0.5%, respectively.

The DSC peaks of *lc*PET and *bo*PET correspond well with other published work.<sup>25,27,28</sup> For example, Karagiannidis et al.<sup>25</sup> reported that, for PET with degree of crystallinity values higher than 30% (i.e., similar to *bo*PET), peaks corresponding to  $T_g$  and cold crystallization in DSC first heating scans were not observed.

**Effect of Temperature and pH on Cutinase-Catalyzed PET Hydrolysis.** Details of methods for purification and characterization of the three cutinases used herein are given in the companion paper.<sup>24</sup> This showed that HiC, PmC, and FsC used herein were highly pure ( $97 \pm 0.4\%$ ,  $99 \pm 0.2\%$ , and  $96 \pm 2\%$ , respectively). Common to previous studies where cutinases were used for polyester hydrolysis reactions, cutinase concentration was not given. Instead, the amount of cutinase used in the reactions was characterized by their activity for the release of *p*-nitrophenol (*p*NP) from *p*NP esters of short-chain fatty acids. Subsequently, on the basis of the activity of cutinases on these model substrates, their activities were compared for polymer hydrolysis reactions.<sup>4,7,8,22</sup> Not surprisingly, Heumann et al.<sup>3</sup> showed that there was no correlation between cutinase activity on *p*NP esters and their activity for the hydrolysis of PET. Thus, in this study, rather than quantifying enzymes by activity units on a surrogate substrate, concentrations of purified cutinases are given in moles per milliliter.

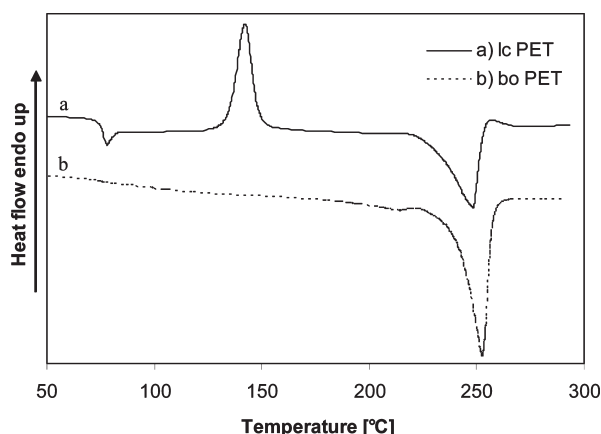


**Figure 1.** DSC thermograms of (a) *lc*PET and (b) *bo*PET, recorded during first heating scans with a heating rate of 10 °C/min.

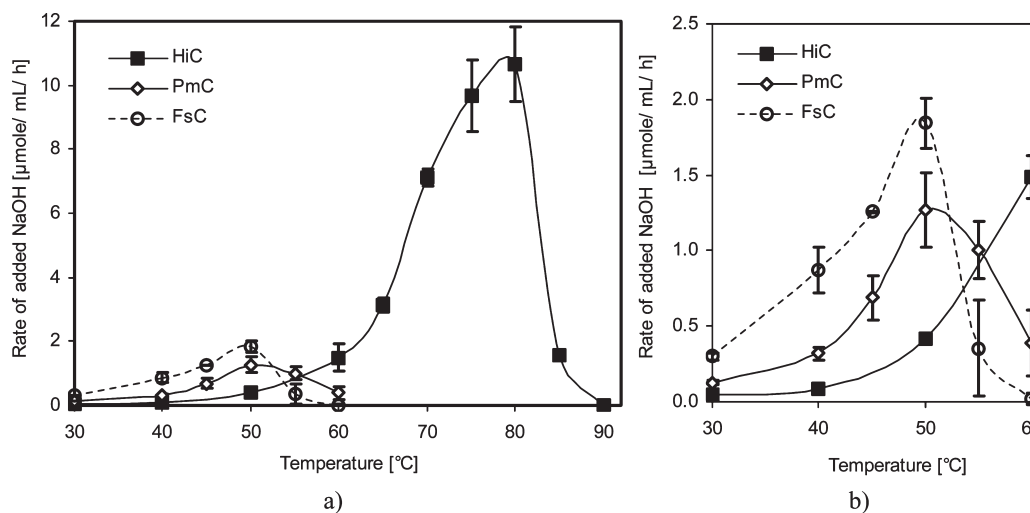


**Figure 2.** Temperature dependence of cutinase activity for *lc*PET hydrolysis at pH 8.0 determined by pH-stat, using 10 mM NaOH as a titrant, with 13 cm<sup>2</sup>/mL of *lc*PET and 6 nmol/mL of cutinase in 3 mL of a 0.5 mM Tris buffer containing 10% glycerol. Graph b is an expansion of the 30–60 °C temperature region in graph a. Error bars represent the standard deviation method based on duplicate repeats.

Cutinase activity for PET hydrolysis was assayed using a pH-stat to measure NaOH consumption versus time. Titration of NaOH by pH-stat keeps the pH constant as acid is liberated due to cutinase-catalyzed PET hydrolysis. Initial slopes in micromoles of NaOH titrated per hour were recorded by pH-stat during the first hour of incubation, and these slope values were used in subsequent plots to assess cutinase activity as a function of incubation parameters (e.g., temperature, pH). Typical plots of NaOH titrated versus time are given in the Supporting Information (Figure S-1). Normally, slopes were measured for lines generated between 15 and 30 min with linear regression ( $R^2$ ) values  $\geq 0.97$ . Figure 2a and b shows the effect of temperature on cutinase initial activity on *lc*PET at a pH of 8.0. As the temperature increases from 30 to 80 °C, HiC activity increases almost 30 fold to 10.6  $\mu\text{mol/mL/h}$ . Thereafter, HiC activity drops steeply to 0 at 90 °C, likely due to thermal-induced denaturation. Figure 2b shows that, at 50 °C, both PmC and FsC reach their maximum activities of 1.3 and 1.8  $\mu\text{mol mL/h}$ , respectively. PmC and FsC lose all activity at about 60 °C; hence, their thermal stabilities are substantially lower than those of HiC.

Further inspection of temperature-dependent HiC-catalyzed *lc*PET hydrolysis results (Figure 2a) shows that hydrolysis activity dramatically increased at temperatures above 65 °C. This is explained by HiC's high thermal stability, which allows incubations of HiC with *lc*PET to be conducted at temperatures nearby *lc*PET's  $T_g$  (75 °C). Welzel's Ph.D. thesis<sup>14</sup> demonstrated that amorphous phase mobility influences polyester biodegradability. Furthermore, Welzel<sup>14</sup> showed that, in order to enable the degradation of aromatic polyesters such as PET, the degradation temperature should be close to its  $T_g$ . Indeed, Müller et al.<sup>11</sup> attributed reaching 50% PET film (surface area of 2.25 cm<sup>2</sup>) weight loss during incubations with *T. fusca* cutinase to its low crystallinity (10%). This enabled degradations at 55 °C, a temperature above that used in previous cutinase-catalyzed PET hydrolysis studies.<sup>3,5,7,8</sup>

The effect of pH on initial HiC, PmC, and FsC activities at 50 °C, and HiC activity at 80 °C, are illustrated in Figure 3a and b, respectively. The activity of FsC is largely unchanged between pH 6.5 and 8.5 (1.9–1.6  $\mu\text{mol/mL/h}$ ) but drops sharply to 0.2 at pH 9.0. Hence, FsC shows poor stability at alkaline pH values of  $\geq 9.0$ . In contrast, PmC activity



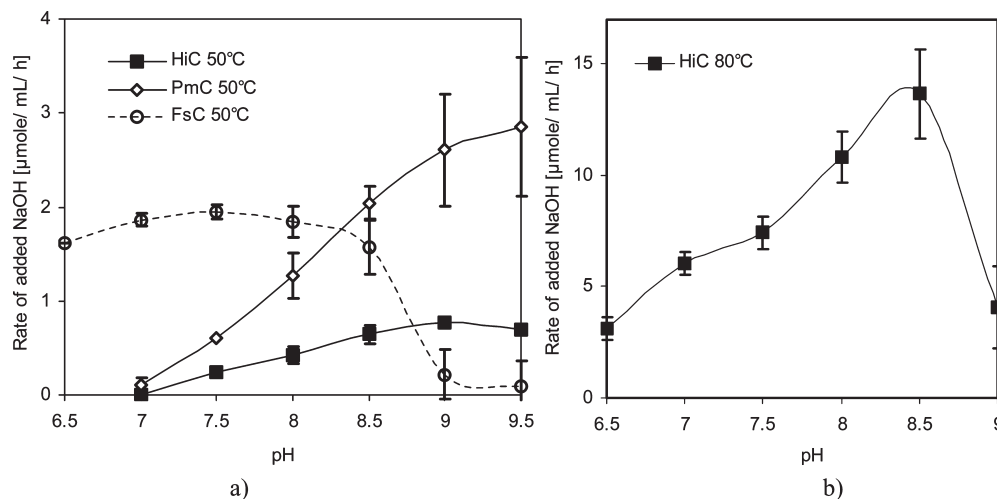


**Figure 3.** Activity of cutinase for *l*PET hydrolysis determined by pH-stat, using 10 mM NaOH as a titrant, with 13 cm<sup>2</sup>/mL of *l*PET and 6 nmol/mL of cutinase in 3 mL of a 0.5 mM Tris buffer containing 10% glycerol. Part a displays the pH dependence at 50 °C for HiC, PmC, and FsC, whereas part b displays pH dependence at 80 °C for HiC. Error bars represent the standard deviation method based on duplicate repeats.

increases from 0.2 to 2.8 μmol/mL/h as the pH is increased from 7.0 to 9.5. Hence, PmC shows exceptional stability under alkaline conditions. HiC shows a similar pH activity trend as PmC at 50 °C since its activity increases from 0.1 to 0.8 μmol/mL/h as the pH is increased from 7.0 to 9.5. A study of Figure 2b along with a comparison between parts a and b of Figure 3 further emphasize the relatively low activity of HiC at 50 °C relative to its activity at 70 and 80 °C. Figure 3b shows that, at 80 °C and pH 8.5, HiC reaches its maximum initial activity of 13.6 μmol/mL/h. However, unlike at 50 °C, an increase in medium pH from 8.5 to 9.0 results in a large decrease in initial activity to 4.1 μmol/mL/h. Hence, HiC's tolerance to pH values ≥ 9.0 is decreased by increases in the medium temperature.

The following discussion compares pH-activity profiles found herein for *l*PET hydrolysis at 50 °C to those reported in the companion paper<sup>24</sup> for cutinase-catalyzed PVAc hydrolysis at 40 °C. Unlike the sizable increases in HiC activity that occurred from pH 7 to 9 for *l*PET hydrolysis, HiC showed little change in activity for PVAc hydrolysis from pH 6.5 to 9.0 at 40 °C. For PmC- and FsC-catalyzed PVAc hydrolysis, activity maxima were observed at pH 8.5 and 9.0, respectively. In contrast, for *l*PET, PmC activity increases to pH 9.5 and FsC activity decreases sharply at pH 9.0. Thus, for all three cutinases, clear differences in pH-activity profiles as a function of the substrate studied were observed. One contributing factor to these dissimilarities may be that investigations for PVAc and *l*PET were conducted at 40 and 50 °C, respectively. Although it was our intent to conduct studies with *l*PET at 40 °C, the low activity of PmC and HiC for *l*PET at 40 °C made this impossible using the pH-stat. Since no previous reports on pH-activity profiles were found for HiC and PmC, comparisons to literature results cannot be made. However, the activity and stability of FsC has been investigated by others. For example, Melo et al.<sup>29</sup> used changes in UV absorbance corresponding to changes in interactions between FsC tyrosine residues to investigate pH effects on FsC denaturation. They showed that, at 50 °C, FsC unfolds at pH 9.6, whereas at 40 °C, FsC unfolds at pH 10.6. Indeed, this result by Melo et al.<sup>29</sup> is in good agreement with studies herein on *l*PET at 50 °C where activity was lost at pH 9.5. This is also consistent with the higher retention of FsC activity on PVAc as the pH was increased from 8.5 to 9 at 40 °C relative to the sharp drop in FsC activity on *l*PET when the pH was increased from 8.5

to 9.0 at 50 °C. Furthermore, Petersen et al.<sup>30</sup> studied the thermal stability of FsC as a function of pH by DSC analysis. They showed maximum stability in the pH range 6–8.5. Thereafter, the stability decayed rapidly at pH values below 6 and above 8.5.<sup>30</sup> This result is similar to that observed for FsC at 50 °C with *l*PET, as FsC activity shows little variation from pH 6.5 to 8.5, but then drops sharply at pH 9.0.

Temperature–activity profiles found herein and that are reported in the companion paper<sup>24</sup> were also compared. As discussed above, an increase in the incubation temperature from 30 to 80 °C increases the activity of HiC for *l*PET hydrolysis almost 30 fold. In contrast, over this same temperature range, HiC activity for PVAc hydrolysis increased only 3.8 fold. This large dissimilarity in temperature–activity behavior is explained by *l*PET experiencing a sizable increase in chain mobility as the temperature is increased to *l*PET's *T<sub>g</sub>* value (75 °C). In contrast, there is no phase transition for PVAc that results in dramatic increases in chain mobility over the temperature range studied. This is due to PVAc's *T<sub>g</sub>* being 32 °C, the lower range of temperatures investigated, and PVAc is amorphous.<sup>31</sup> PmC and FsC temperature–activity profiles appear similar herein to that described in ref 24 using PVAc. The only difference is a slight increase in FsC thermal stability, from 40 to 45 °C with PVAc to 50 °C with *l*PET. It is noteworthy that temperature–activity profiles were determined at pH 7.5 and 8.0 for PVAc and *l*PET, respectively. Since both pH values are well within the range where all three cutinases are stable, it is unlikely that this small difference in pH plays a significant role in the above temperature–activity comparisons.

**Influence of Crystallinity.** To investigate the influence of PET crystallinity on HiC, PmC, and FsC activity, comparisons were made using *l*PET and *bo*PET (see above). Observation of Figure 4 shows that initial activities of HiC, PmC, and FsC decreased 25-, 10-, and 6-fold when exposed to PET films of higher crystallinity (35 vs 7%). This is consistent with results reported by many other investigators who studied how alteration in polyester crystallinity influences hydrolytic enzyme activity.<sup>19,20,32–35</sup> Vertommen et al.<sup>7</sup> showed that FsC displayed higher hydrolytic activity toward amorphous PET than crystalline PET (4% versus 48% crystallinity). Marten et al.<sup>15</sup> showed that, in order to improve the biodegradation rate for crystalline or semicrystalline polyesters, enzyme-polymer incubations should be

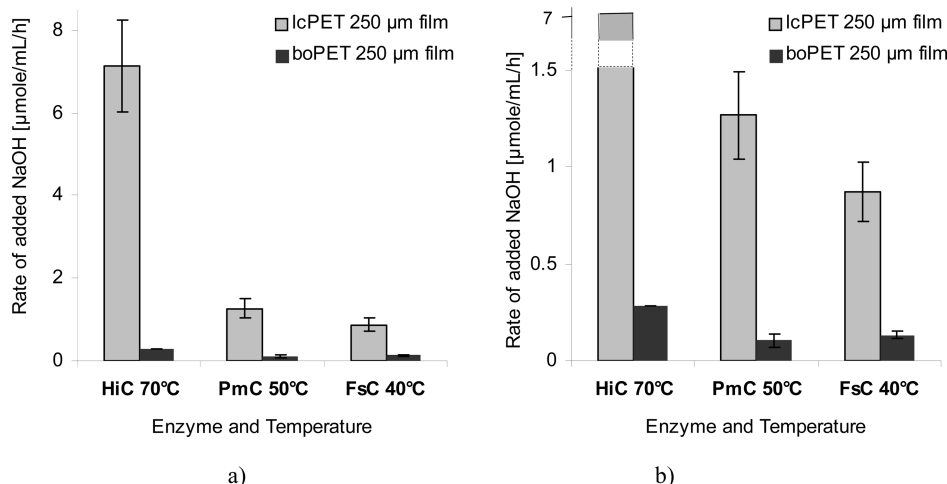


**Figure 4.** Effect of crystallinity on cutinase-catalyzed hydrolysis of PET at pH 8.0, determined by pH-stat, using 10 mM NaOH as a titrant, with 13 cm<sup>2</sup>/mL of either *l*cPET (7% crystallinity) or *h*oPET (35 crystallinity) and 0.13 mg/mL of either HiC, PmC, or FsC at 70, 50, and 40 °C, respectively. Graph b is an expansion of the y axis in graph a from 0 to 1.5 μmol/mL/h. Error bars represent the standard deviation method based on duplicate repeats.

performed close to the polymer's melting point. However, since PET's melting point (250 °C) is well above temperatures at which enzymes are stable, this strategy cannot currently be employed for PET with a high crystalline content.

Further study of Figure 4 shows that, when *l*cPET is the substrate, HiC exhibits a 6-fold higher initial rate relative to PmC and FsC. When *h*oPET is the substrate, HiC has about 2-fold higher hydrolytic activity relative to PmC and FsC. As discussed above, the importance of being able to conduct enzyme-PET incubations near or above its  $T_g$  cannot be overemphasized. Interestingly, comparison of activities of HiC, PmC, and FsC at 50 °C (pH 8.0, see Figure 2b) on *l*cPET show that their initial rates are 0.42, 1.27, and 1.84 mM h<sup>-1</sup>, respectively. In other words, if restricted to lower-temperature conditions, HiC would not be the preferred enzyme for PET hydrolysis. By remaining active at PET's  $T_g$ , HiC has the advantage of access to more mobile chains in the amorphous phase. Thus, the observed higher activity of HiC compared to that of FsC and PmC under optimal temperature–pH conditions appears to be largely a function of physical changes occurring in PET at its  $T_g$ .

In kinetic studies described below with HiC, PmC, and FsC, cutinase–*l*cPET incubations were conducted at pH 8.0 and at 70, 50, and 40 °C, respectively. Hence, although FsC showed maximum initial activity at 50 °C (Figure 2), its poor thermal stability, demonstrated in the companion paper,<sup>24</sup> suggested that working at a lower temperature is advised. Furthermore, the decision to carry out kinetic studies with HiC at 70 instead of 80 °C was made to reduce the magnitude of uncertainty in the measurements (see error bars in Figure 1a at 70, 80, and 90 °C) as well as to reduce water evaporation during long-term incubations. Moreover, instead of maintaining the pH at 8.5 for PmC and HiC, all three cutinases were studied at a pH of 8.0 to reduce background chemical hydrolysis while supporting high cutinase activity.

**Kinetic Studies.** The classical Michaelis–Menten enzyme kinetic model, derived for homogeneous reactions, is based on enzyme-limited conditions. However, in the case of enzymatic polymer degradation where the substrate is usually insoluble and the reaction is limited to the surface of the substrate (substrate-limited), the Michaelis–Menten model will generally not apply. Alternative heterogeneous kinetics models based on substrate-limited conditions have therefore been

developed for (i) poly( $\beta$ -hydroxybutyrate) (PHB)-depolymerase-catalyzed poly(3-hydroxybutyrate) hydrolysis,<sup>36–39</sup> (ii) lipase-catalyzed PCL hydrolysis, (iii) lipase-catalyzed hydrolysis of polyester nanoparticles,<sup>14,40,41</sup> and (iv) cellulase-catalyzed hydrolysis of cellulose.<sup>42–44</sup> Mukai et al.<sup>37</sup> proposed a kinetic model for PHB-depolymerase-catalyzed hydrolysis of PHB to account for enzyme–substrate heterogeneity as well as different roles played by enzyme binding and active sites. This model was later modified by Timmins and Lenz<sup>36</sup> in order to account for substrate concentration. Subsequently, Scandola et al.<sup>39</sup> demonstrated that the same enzymatic degradation could be expressed by a two-step kinetic model with the following initial reaction rate ( $V_0$ ) equation:

$$V_0 = k_2[S]_0 \frac{K[E]_0}{K + [E]_0} \quad (2)$$

or as a linearized expression:

$$\frac{[S]_0}{V_0} = \frac{1}{Kk_2[E]_0} + \frac{1}{k_2} \quad (3)$$

where  $[S]_0$  is the initial surface concentration,  $[E]_0$  is the initial enzyme concentration, and  $k_2$  is the hydrolysis rate constant. Also,  $K$  is the adsorption equilibrium constant defined as the ratio of the rate constant for adsorption to that for desorption ( $k_1/k_{-1}$ ). Interestingly, the rate equations from the kinetic models referred to above for lipases<sup>14,40,41</sup> and cellulases<sup>42–44</sup> are expressed similarly as eq 2, but where the constants are defined differently. Herzog et al.<sup>41</sup> developed a rate equation for the lipase-catalyzed hydrolysis of polyester nanoparticles. Like eq 2, they assumed that the degradation rate is proportional to the surface area, but they also introduced the idea that the molar density of ester bonds of the polymer, and enzyme loading at the polymer surface, are proportional to the degradation rate. The rate equation they proposed to describe enzymatic polyester hydrolysis takes into account important variables that undoubtedly influence the degradation rate. However, by introducing two additional variables, the equation becomes more complicated to solve and requires further information about the system under study. Herzog et al.<sup>41</sup> solved for these two variables by introducing an equation that describes the conversion of cleaved ester bonds as a function of time until the reaction reaches a plateau value.

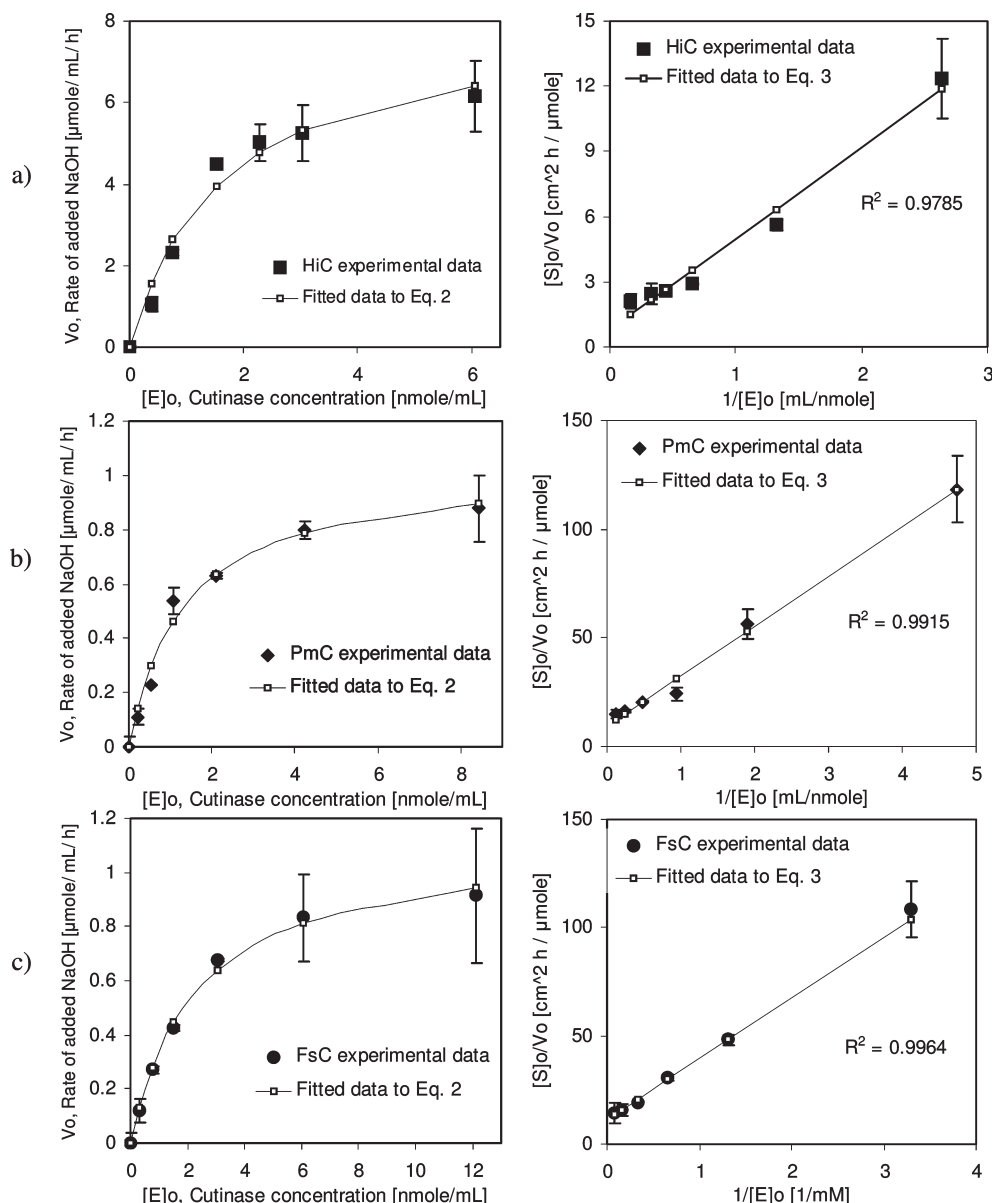


**Figure 5.** Initial rate of NaOH consumption as a function of cutinase concentration and reciprocal plots based on eq 3, shown on the left and right sides, respectively. Experiments were performed with HiC, PmC, and FsC at 70, 50, and 40 °C, respectively, with the *lc*PET concentration fixed at 13  $\text{cm}^2/\text{mL}$ . Experimental values are plotted as filled symbols, whereas data fitted to eqs 2 and 3 are shown as solid lines on the left and right sides, respectively. Error bars represent the standard deviation method based on duplicate repeats.

While evaluation of how experimental data obtained herein would fit rate expressions developed by Herzog et al.<sup>41</sup> is of great interest and was strongly considered, further study led us to conclude that this evaluation could not be performed with the current system. That is, the Herzog rate equations require rapid polyester hydrolysis, which was achieved by using an aliphatic polyester substrate with a high available surface area resulting from nanoparticle formation. In contrast, *lc*PET degrades relatively slowly, and its surface area is limited since it is used in film form. Therefore, the kinetic study presented below was performed by applying eqs 2 and 3.

The pH-stat assay was used to determine the dependence of the *lc*PET hydrolysis rate on cutinase concentration. Concentrations of the three cutinases were varied at a fixed PET surface concentration (13  $\text{cm}^2/\text{mL}$ ). Incubations were performed for 1 h in a 0.5 mM Tris-HCl buffer (3 mL, pH 8) with 10% glycerol, at 70, 50, and 40 °C for HiC, PmC, and FsC, respectively. Plots of experimental enzymatic hydrolysis rates versus enzyme concentration are displayed in

Figure 5 (left side). Initial hydrolysis rates were determined from linear slopes of NaOH versus time data (see Figure S-2, Supporting Information). Experimental data points are shown as filled symbols, whereas, theoretical results from equation fitting are shown as solid lines. The right side of Figure 5 presents reciprocal plots based on eq 3. It is observed that the hydrolysis rate dependence of  $[E]_o$  changes from first- to zero-order kinetics. The maximum rates reached by HiC, PmC, and FsC are 6.1, 0.8, and 0.9  $\mu\text{mol/mL/h}$ , respectively. Using the Solver utility in Excel for Windows, values for parameters  $K$  and  $k_2$  were found by fitting eq 2 to experimental data by a least mean-square regression fit. The results are shown as solid lines on the left side of Figure 5. Similarly, eq 3 was fit to the experimental data by applying the calculated  $K$  and  $k_2$  from eq 2 as input. The reciprocal form of this data and the corresponding values of  $R^2$  in Figure 5 (right side) verify the linearity of experimental data. Furthermore, agreement between experimental data plotted in the reciprocal form suggested by eq 3

**Table 1. Kinetic Parameters from eq 2 Determined for PET Hydrolysis Using HiC, PmC, and FsC at 70, 50, and 40 °C, Respectively**

	$[S]_0$ ( $\mu\text{M}$ )	$K$ ( $\mu\text{M}^{-1}$ )	$k_2$ ( $\mu\text{mol}/\text{cm}^2/\text{h}$ )
HiC	13	0.64	0.62
PmC	13	0.76	0.08
FsC	13	0.41	0.09

and corresponding fitted plots using eq 2 show that hydrolysis of *lc*PET, using HiC, PmC, and FsC, obeys the kinetic model proposed by Scandola et al.<sup>39</sup>

The kinetic parameters determined from eq 2 for HiC, PmC, and FsC are shown in Table 1. HiC at 70 °C has the highest hydrolysis rate constant,  $k_2$  ( $0.62 \mu\text{mol}/\text{cm}^2/\text{h}$ ), which is 7-fold higher than rates of PmC and FsC at 50 and 40 °C, respectively. Interestingly, this corresponds to observations in the temperature study (Figure 2) where HiC at 70 °C showed 6-fold higher activity than PmC at 50 °C and FsC at 40 °C. Further study of Figure 2 shows that PmC and FsC have similar hydrolytic activities at 50 and 40 °C, respectively. Also, the  $k_2$  results in Table 1 for PmC and FsC are close in value ( $0.08$  and  $0.09 \mu\text{mol}/\text{cm}^2/\text{h}$ , respectively). The adsorption constant  $K$  shown in Table 1 is a measure of the enzymes' affinity to *lc*PET. Though the three cutinases show similar  $K$  values, PmC has the highest affinity to PET, while FsC possesses the lowest affinity. Interestingly, the same observation was made in our companion paper,<sup>24</sup> where PmC showed the highest affinity to PVAc while FsC showed the lowest. However, in PVAc hydrolysis, differences in cutinase affinities were larger in magnitude.

Figure 6 shows the initial hydrolysis rate data measured by NaOH consumption as a function of *lc*PET concentration. Concentrations of HiC, PmC, and FsC were held constant at 2, 2, and 3 nmol/mL, respectively. The cutinase concentrations selected were at the higher end of those within the linear region of  $V_0$  versus  $E_0$  plots, so that reactions were still under substrate-saturated conditions. Experimental hydrolysis rates of *lc*PET are shown as filled symbols and solid lines in Figure 6.

They reveal a linear dependency on  $[S]_0$  up to 15, 20, and 20  $\text{cm}^2/\text{mL}$  for HiC, PmC, and FsC, respectively. Taking values of  $K$  and  $k_2$  from Table 1, eq 2 was used to generate a plot of  $V_0$  as a function of  $[S]_0$ , shown as dotted lines in Figure 6. By comparing experimental and fitted data from eq 2, it is concluded that eq 2 is applicable only under substrate-limiting conditions. This confirms that, under conditions where cutinase activity is determined using *lc*PET in film form as a substrate, the kinetic data for all three cutinases, obtained as a function of both enzyme and substrate concentrations, fit the kinetic model proposed by Scandola et al.<sup>39</sup> (eq 2). It would be of interest to perform a similar kinetic analysis using *bo*PET as a substrate. Unfortunately, using the pH-stat method described herein and in the companion paper,<sup>24</sup> the hydrolysis rate was too slow. Thus, for kinetic studies of *bo*PET with the enzymes studied herein, a more sensitive analytic method will be required.

**Long-Term Incubations of Cutinases with PET.** Kinetic and temperature studies were based on results from measured initial rates, determined during the first hour of cutinase–PET incubations. Also of interest is a determination of to what degree the three cutinases are able to degrade the *lc*PET film during extended incubation times. Figure 7 shows weight loss of the *lc*PET film (80 mg with dimensions  $15 \text{ mm}^2 \times 15 \text{ mm}^2 \times 250 \mu\text{m}$ ) as a function of incubation time and cutinase used in 1 M Tris-HCl. Consistent with expectations from kinetic studies above, HiC was most active for the catalysis of *lc*PET hydrolysis. In fact, HiC completely

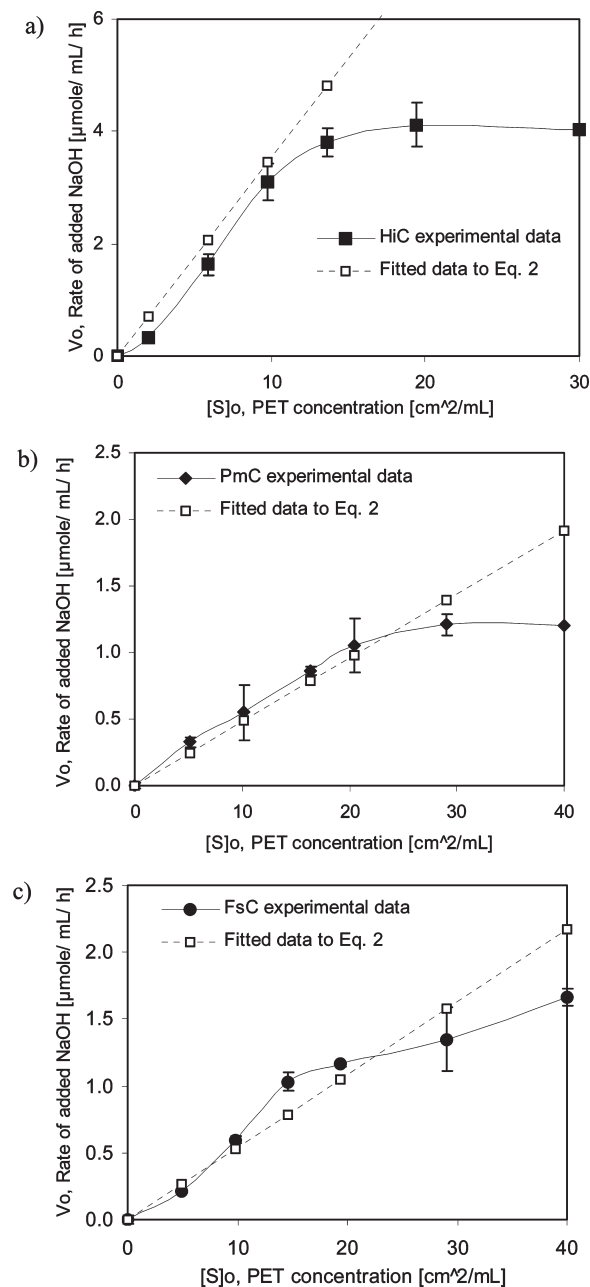


**Figure 6.** Initial rate of NaOH consumption as a function of *lc*PET concentration: (a) 2 nmol/mL HiC at 70 °C, (b) 2 nmol/mL PmC at 50 °C, (c) 3 nmol/mL FsC at 40 °C. Experimental values are plotted as filled symbols and solid curves, whereas plots generated by fitting eq 2 are shown as dotted lines with open symbols. Error bars represent the standard deviation method based on duplicate repeats.

degrades the *lc*PET film ( $97 \pm 3\%$  weight loss) to water-soluble products within 96 h. Taking into account that PET films are about  $250\text{-}\mu\text{m}$ -thick, this represents a degradation rate of  $30 \mu\text{m}$  per day or  $210 \mu\text{m}$  per week (per film side). Regarding enzyme coverage,  $0.09 \text{ mg}$  of enzyme is available per square centimeter. In control studies conducted without HiC, no significant ( $< 1\%$ ) *lc*PET weight loss was observed. In a related study, Müller et al.<sup>11</sup> exposed a low-crystallinity PET film to *T. fusca* cutinase at 55 °C. Available *T. fusca* cutinase was  $0.22 \text{ mg}$  per  $\text{cm}^2$  PET surface. The result was a film weight loss of 50% within three weeks and a thickness decrease rate of  $17 \mu\text{m}$  per week. Furthermore, PET used by Müller et al.<sup>11</sup> had a crystallinity of 9%,  $T_g$  at 75 °C, and a melting temperature at 249 °C. Similarly, *lc*PET used herein



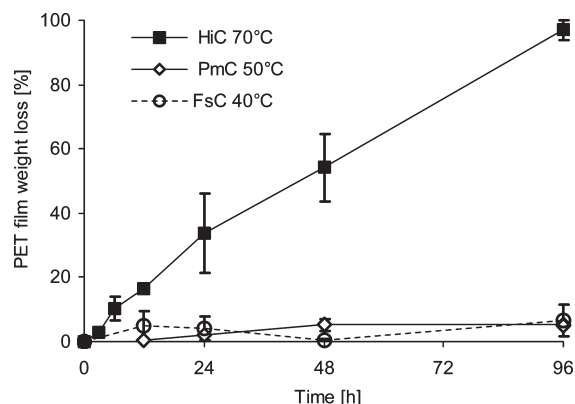


**Figure 7.** Degradation study of *lc*PET (2.25 cm<sup>2</sup>/mL) as a function of incubation time in 1 M Tris-HCl with 10% glycerol, at pH 7.5 and 10 nmol/mL of either HiC, PmC, or FsC at 70, 50, and 40 °C, respectively. Error bars represent the standard deviation method based on triplicate repeats.

has a degree of crystallinity of  $7 \pm 1\%$ ,  $T_g$  at 75 °C, and a melting temperature at 247 °C. Thus, the PET films used in these two studies have similar physical properties. It is therefore concluded that HiC has remarkably higher activity than *T. fusca* cutinase for *lc*PET hydrolysis. This is largely attributable to the higher thermal stability of HiC. Indeed, incubations of HiC with *lc*PET at 70 °C are close to the  $T_g$  of PET. Inspection of Figure 2 shows that, by increasing the incubation temperature of HiC with *lc*PET from 55 to 70 °C, the initial rate of hydrolysis increased 7-fold. Thus, HiC more affectively hydrolyzes PET when its amorphous phase is near, at, or above PET's  $T_g$ , where chains at or nearby the film surface have greater mobility.

Figure 7 also shows the results of *lc*PET incubation with PmC at 50 °C and FsC at 40 °C. For FsC, a  $5 \pm 1\%$  weight loss was reached within the first 24 h, and thereafter, little change in film weight loss was observed. For PmC, film weight loss slowly increased so that, by 48 h, weight loss reached 5%, and no further increase in weight loss was observed to 96 h. The liquid media from both FsC and PmC film incubation studies were separated from films after 96 h. These liquid media were then used to perform weight loss studies with virgin *lc*PET films. Similar weight loss values were reached with the new films ( $\sim 5\%$  within 96 h), suggesting that the attainment of a plateau after which further weight loss was not observed is not attributable to deactivation of the cutinase remaining in the media (not on film surfaces). Vertommen et al.<sup>7</sup> reported that strong adsorption by FsC to PET surfaces occurs. One hypothesis that explains these results is that PmC and FsC saturate available *lc*PET surfaces and, over the course of 24 to 48 h, become deactivated. Soluble cutinase in the media may not have access to enzyme-saturated surfaces, and no further degradation occurs. Further work is planned to investigate the validity of this hypothesis. PmC and FsC, like *T. fusca* cutinase, lack sufficient thermal stability to allow incubations at or above 70 °C. Being 25 to 35 °C below the  $T_g$  of PET is a serious disadvantage, as is discussed above.

It is noteworthy that *bo*PET was similarly exposed for 96 h to HiC, PmC, and FsC at 70, 50, and 40 °C, respectively. However no measurable weight loss was detected with all three cutinases.

The long-term study of HiC catalyzed *lc*PET film weight loss as a function of time (Figure 7) was performed in 1 M Tris buffer. The choice of this buffer strength was based on the desire to maintain medium pH at a value close to that of

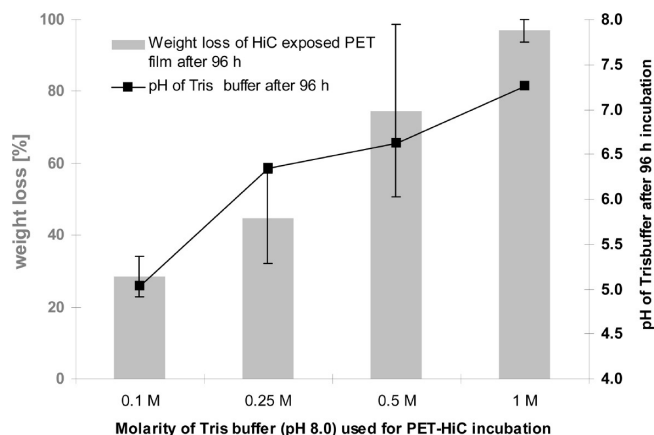


**Figure 8.** (Left axis) *lc*PET film (2.25 cm<sup>2</sup>/mL) weight loss as a function of Tris buffer molarity. The right axis shows the pH of media after 96 h incubations. Incubations were performed at 70 °C, with 10 nmol/mL of HiC, in Tris-HCl (3 mL, pH 8.0) with 10% glycerol. Error bars represent the standard deviation method based on triplicate repeats.

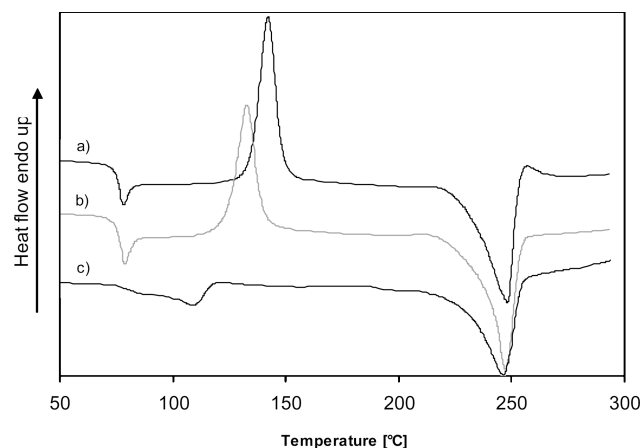


**Figure 9.** DSC thermograms recorded during first heating scans of (a) as-received *lc*PET, (b) *lc*PET incubated without enzyme addition for 96 h at 70 °C in Tris-HCl (pH 8), and (c) recovered film after incubation of *lc*PET for 96 h with HiC in Tris-HCl (pH 8.0) at 70 °C.

the starting pH (8.0). Figure 3, above, shows that HiC activity is highly dependent on medium pH, decreasing regularly as pH decreases below 8.0. The relationship between medium Tris buffer strength, pH decrease during incubations and *lc*PET film weight loss after 96 h incubations with HiC is shown in Figure 8. By using 1 M Tris buffer, the final pH of incubation media was 7.3 and film weight loss was nearly complete. However, for incubations of HiC conducted with Tris buffer concentrations of 0.5, 0.25, and 0.1 M, the final pH in media decreased to pH 6.6, 6.4, and 5.0 respectively, and film weight loss decreased to 75, 45 and 28%, respectively.

Of interest is the extent that *lc*PET crystallinity changes both during exposure to HiC and under control conditions without the enzyme at 70 °C. Figure 9 shows DSC thermograms of *lc*PET recorded during first heating scans: (i) prior to incubations (scan a), (ii) a control, incubated for 96 at 70 °C (scan b), and (iii) recovered PET after exposure to HiC at 70 °C for 96 h (scan c). Analysis of thermogram a shows that the nontreated *lc*PET film has a  $T_g$  at 75 °C, a cold crystallization peak at 142 °C, and a peak melting temperature ( $T_m$ ) at 247 °C. A study of thermogram c, recording the PET recovered after exposure to HiC for 96 h ( $\sim 3\%$  of the starting film weight), shows that the  $T_g$  increases to 80 °C,



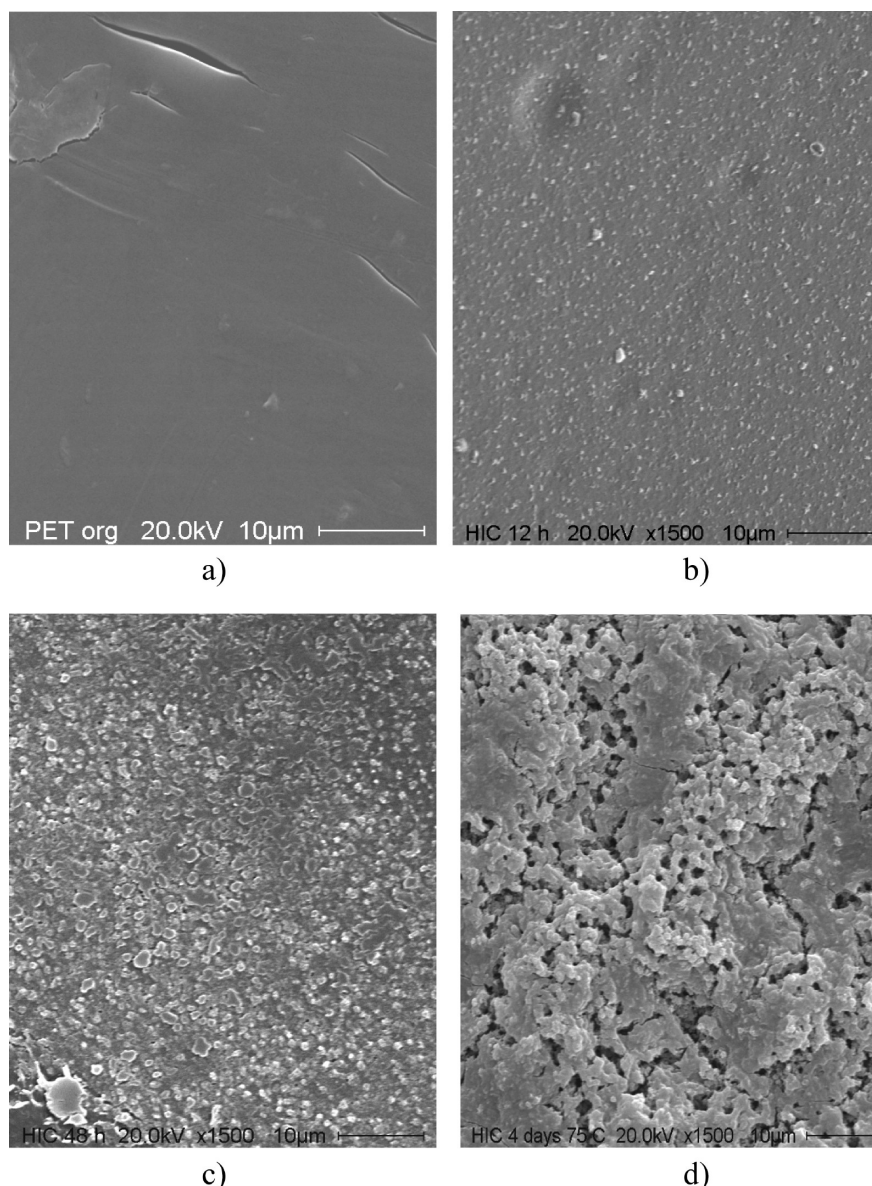


**Figure 10.** SEM images of *l*PET films exposed to HiC for different time periods, resulting in varying extents of film weight loss. The following describes incubation times and % film weight loss values: (a) *l*PET as received, (b) 12 h exposure with 18% weight loss, (c) 48 h exposure with 54% weight loss, (d) 96 h exposure with 95% weight loss.

and the cold crystallization transition is not found. Instead of a crystallization transition, a small premelting endothermic peak<sup>25</sup> appears in about the same temperature region. Furthermore, from analysis of the melting heat of fusion, the crystallinity increased to 27%. Therefore, consistent with results of HiC on *bo*PET (see above), HiC preferentially degrades amorphous regions of the polymeric material. The preferential attack by enzymes of polymer amorphous regions is expected and has been reported by others using various enzyme–polymer systems.<sup>7,10,11,19,20,32–35,45</sup> Of six replicate experiments where *l*PET was exposed to HiC for 96 h at 70 °C, two of these runs resulted in complete conversion of the film to water-soluble products (e.g., 100% film weight loss). Thus, although HiC is more active on amorphous regions of PET, it has sufficient activity on crystalline domains to completely degrade *l*PET. Another important question was whether the *l*PET crystallinity increases under control conditions when heated without an enzyme at 70 °C for 96 h. Recovery of the film after this control experiment and analysis of crystallinity by DSC

shows only a small increase to 9%. This minor rise in crystallinity is also evident by a shift of the cold crystallization peak to lower temperatures compared to the initial sample, a phenomenon known to occur for even small changes in crystallinity.<sup>26</sup>

The effect on surface roughness caused by the incubation of HiC with a *l*PET film was studied by recording SEM photographs, displayed in Figure 10. Inspection of the SEM images shows that, as incubation time was increased from 12 to 48 and 96 h corresponding to weight loss values of 18, 54, and 95%, surface roughness increases so that, at 96 h, the recovered film surface has holes of up to 5  $\mu$ m penetrating below the surface.

**Analysis of Degradation Products.** The separation of TPA, BHET, and MHET was achieved by HPLC using a reversed-phase column run under isocratic conditions with UV detection (see Materials and Methods section and chromatograms *a* and *b* in Figure 11). This allowed construction of calibration curves for these compounds from 0.5 to 25  $\mu$ g/mL with  $R^2$  values of 0.997.

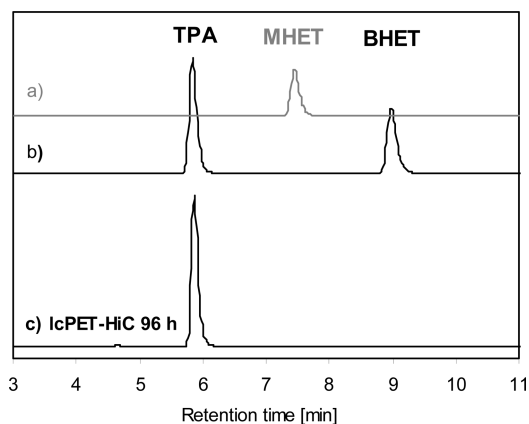


**Figure 11.** HPLC chromatogram *c*: the hydrolysis product (TPA) generated by HiC-catalyzed hydrolysis of *lcpET* ( $2.25 \text{ cm}^2/\text{mL}$ ) by  $10 \text{ nmol/mL}$  of HiC in  $1 \text{ M}$  Tris-HCl with  $10\%$  glycerol ( $\text{pH } 8.0$ ,  $70^\circ\text{C}$ ). Chromatograms *a* and *b* show retention times of TPA, MHET, and BHET standards prepared for this analysis.

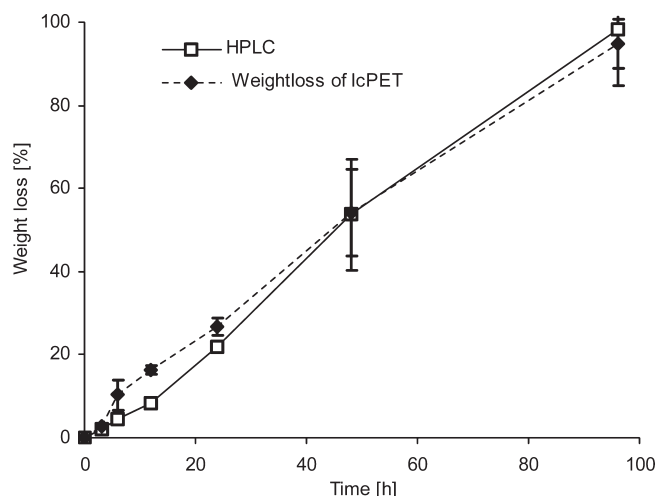


**Figure 12.** Comparison of *lcpET* film weight loss determined by measuring TPA concentration accumulated in media and by direct gravimetric measurements to determine film weight loss for incubations with  $10 \text{ nmol/mL}$  of HiC in  $1 \text{ M}$  Tris-HCl with  $10\%$  glycerol at  $70^\circ\text{C}$  and  $\text{pH } 8.0$ . Error bars represent the standard deviation method based on triplicate repeats.

Figure 11c shows the HPLC chromatogram obtained by analyzing the medium after a 96 h incubation of *lcpET* with HiC in  $1 \text{ M}$  Tris-HCl ( $\text{pH } 8$ ) at  $70^\circ\text{C}$ . The only compound found is TPA. Similarly, only TPA was found when the same HPLC analysis was performed on media from incubations of *lcpET* with PmC and FsC for 96 h, corresponding to film weight loss values of 5% for both enzymes. In contrast, Yoon et al.<sup>5</sup> reported that, in addition to TPA, treatment of PET fibers with PmC produced unidentified terephthalate-containing species, whereas NaOH-treated PET fibers yielded only TPA. Vertommen et al.<sup>7</sup> found that FsC-catalyzed PET hydrolysis predominantly produced MHET, some TPA, and small traces of BHET. They also reported that the ratio of MHET to TPA depended on the ratio of cutinase to PET. The smaller the ratio of enzyme to substrate, the more predominant MHET became. Relative to studies carried out herein, previous work discussed in refs 5 and 7 was conducted with differences in the reaction temperature, buffer, and ratio of cutinase to substrate. Such changes in incubation conditions could lead to incomplete conversion

of water-soluble PET degradation products to TPA. However, our study shows definitively that, under the appropriate conditions, HiC, FsC, and PmC are all active for complete conversion of *lcpET* to TPA and ethylene glycol.

On the basis of the above discovery that TPA is the only degradation product that accumulates in media during HiC-catalyzed degradation of *lcpET*, the TPA concentration in media determined by HPLC analysis as a function of incubation time was used to predict the extent of *lcpET* film weight loss that occurred during incubations with HiC at  $70^\circ\text{C}$  and  $\text{pH } 8$ . Values of film weight loss determined by measuring the mass change of films and calculated on the basis of a HPLC analysis of TPA in incubation media were in excellent agreement (see Figure 12). This comparison validates the HPLC method used, along with the conclusion that TPA is the predominant degradation product formed from the cutinase-catalyzed hydrolysis of *lcpET*. Furthermore, the results herein show the potential of using cutinases for conversion of PET to high-purity TPA and ethylene glycol.

## Conclusions

This paper compares the activity of three different cutinases in purified form, notably, HiC, PmC, and FsC, using PET with low (*lc*, 7%) and higher (*hc*, 35%) crystallinity. Consistent with previous reports by others using different enzyme-polymer systems,<sup>17,19,20,32–35,45</sup> increased PET crystallinity negatively affects cutinase's ability to degrade PET. Initial activities of cutinase on *lcpET* were successfully fit to a heterogeneous kinetic model. This provides an opportunity to quantitatively compare HiC, PmC, and FsC while gaining a better understanding of fundamental differences in their kinetic parameters. For example, results herein revealed that PmC and FsC had the highest and lowest affinities, respectively, for *lcpET*. Furthermore, the initial hydrolysis rate of HiC is 7-fold higher than PmC and FsC. The reason for HiC's remarkable activity for *lcpET* hydrolysis was largely attributed to its ability to remain active at  $70^\circ\text{C}$ , just below PET's  $T_g$ . At this temperature, HiC benefits from higher mobility of the chains in the amorphous phase, thus increasing the accessibility of HiC to PET ester groups. Results from initial degradation rates were consistent with extended time incubations of cutinases with *lcpET*. Thus, incubations of 96 h duration at  $70^\circ\text{C}$  of HiC with *lcpET* resulted in a  $97 \pm 3\%$  film weight loss. In contrast, 96 h incubations of *lcpET* with PmC and FsC at 50 and  $40^\circ\text{C}$ , respectively, resulted in a 5% weight loss. Nevertheless, PmC and FsC remain of great interest for performing surface modification of PET used in textile and biomedical applications where the goal is to increase surface hydrophilicity that requires little or no PET weight loss. Indeed, previous studies by others have demonstrated the utility of PmC and FsC for increasing PET surface hydrophilicity.<sup>3–8</sup> Results herein show that HiC's activity for *lcpET* hydrolysis is much higher than was previously reported,<sup>11</sup> and HiC was found to remain active over extended times to completely degrade films that are  $250\text{-}\mu\text{m}$ -thick. Furthermore, all three cutinases degrade PET to TPA. Thus, the potential to completely convert commercial PET materials of low crystallinity to TPA and ethylene glycol under mild conditions was demonstrated. Indeed, the majority of PET recycling is focused on the bottle manufacturing industry, which utilizes PET of low crystallinity to achieve high bottle transparency.<sup>11</sup>

**Acknowledgment.** We thank the National Science Foundation Industry/University Cooperative Research Center (NSF-I/UCRC) for Biocatalysis and Bioprocessing of Macromolecules at Polytechnic Institute of NYU for their financial support, intellectual input, and encouragement during the course of this research.



**Supporting Information Available:** Titration plots from the pH-stat study of cutinase catalyzed PET hydrolysis are given. Typical plots of NaOH titrated versus time are given as function of temperature (Figure S-1), cutinase concentration (Figure S-2), and substrate concentration (Figure S-3). This information is available free of charge via the Internet at <http://pubs.acs.org>.

## References and Notes

- Guebitz, G.; Cavaco-Paulo, A. Enzyme go big: surface hydrolysis and functionalisation of synthetic polymers. *Trends Biotechnol.* **2007**, *26* (1), 32–38.
- Fischer-Colbrie, G.; Heumann, S.; Guebitz, G. Enzyme for polymer surface modification. In *Modified fibers with medical and specialty applications*; Edwards, J. V., Buschle-Diller, G., Goheen, S. C., Eds.; Springer: New York, 2006; Vol. 8, pp 125–143.
- Heumann, S.; Eberl, A.; Pobeheim, H.; Liebinger, S.; Fischer-Colbrie, G.; Almansa, E.; Cavaco-Paulo, A.; Guebitz, G. M. New model substrates for enzymes hydrolysing polyethyleneterephthalate and polyamide fibres. *J. Biochem. Biophys. Methods* **2006**, *39*, 89–99.
- Alisch, M.; Feuerhack, A.; Muller, H.; Mensak, B.; Andreus, J.; Zimmermann, W. Biocatalytic Modification of Polyethylene Terephthalate Fibers by Esterases from Actinomycete Isolates. *Biocatal. Biotransform.* **2004**, *22* (5/6), 347–351.
- Yoon, M. Y.; Kellis, J. T.; Poulouse, A. J. Enzymatic modification of polyester. *AATCC Rev.* **2002**, *2* (6), 33–36.
- Kellis, J. T.; Poulouse, A. J.; Yoon, M. Y. Enzymatic modification of the surface of a polyester fiber or article. U.S. Patent 6,254,645 B1, **2001**.
- Vertommen, M. A. M. E.; Nierstras, V. A.; van der Veer, M.; Warmoeskerken, M. M. C. G. Enzymatic surface modification of poly(ethylene terephthalate). *J. Biotechnol.* **2005**, *120*, 376–386.
- Araújo, R.; Silva, C.; O'Neill, A.; Micaelo, N. M.; Guebitz, G.; Soares, C. M.; Casal, M.; Cavaco-Paulo, A. Tailoring cutinase activity towards polyethylene terephthalate and polyamide 6,6 fibers. *J. Biotechnol.* **2007**, *128*, 849–857.
- Eberl, A.; Heumann, S.; Kotek, R.; Kaufmann, F.; Mitsche, S.; Cavaco-Paulo, A.; Guebitz, G. M. Enzymatic hydrolysis of PTT polymers and oligomers. *J. Biotechnol.* **2008**, *135*, 45–51.
- Mueller, R.-J. Biological degradation of synthetic polyesters - Enzymes as potential catalysts for polyester recycling. *Process Biochem.* **2006**, *41*, 2124–2128.
- Müller, R.-J.; Schrader, H.; Profe, J.; Dresler, K.; Deckwer, W.-D. Enzymatic Degradation of Poly(ethylene terephthalate): Rapid hydrolyse using a hydrolase from *T. fusca*. *Macromol. Rapid Commun.* **2005**, *26*, 1400–1405.
- Mueller, R.-J.; Kleeberg, I.; Deckwer, W.-D. Biodegradation of polyesters containing aromatic constituents. *J. Biotechnol.* **2001**, *86*, 87–95.
- Gallagher, F. G. Controlled degradation polyesters. In *Modern Polyesters: chemistry and technology of polyesters and copolyesters*; Scheirs, J., Long, T. E., Eds.; John Wiley & Sons: New York, 2003; pp 591–608.
- Welzel. Einfluss der chemischen Struktur auf die enzymatische Hydrolyse von Polyester-Nanopartikeln; TU Braunschweig: Braunschweig, Germany, 2003.
- Marten, E.; Muller, R.-J.; Deckwer, W.-D. Studies on the enzymatic hydrolysis of polyesters I. Low molecular mass model esters and aliphatic polyesters. *Polym. Degrad. Stab.* **2003**, *80*, 485–501.
- Gross, R. A.; Kalra, B. Biodegradable polymers for the environments. *Science* **2002**, *297*, 803–807.
- Parikh, M.; Gross, R. A.; McCarthy, S. P., The effect of crystalline morphology on enzymatic degradation kinetics. In *Biodegradable polymers and packaging*; Ching, C., Kaplan, D. L., Thomas, E. L., Eds.; Technomic: Lancaster-Basel, 1993; pp 407–415.
- Tokiwa, Y.; Suzuki, T. Hydrolysis of copolyesters containing aromatic and aliphatic ester blocks by lipase. *J. Appl. Polym. Sci.* **1981**, *26*, 441–448.
- Huang, S. J. Biodegradation. *Compr. Polym. Sci.* **1989**, *6*, 597–606.
- Nishida, H.; Tokiwa, Y. Effects of higher-order structure of Poly(3-hydroxybutyrate) on biodegradation. II Effects of crystall structure on microbial degradation. *J. Environ. Polym. Degrad.* **1993**, *1* (1), 65–80.
- Witt, U.; Mueller, R.-J.; Deckwer, W.-D. New biodegradable polyester-copolymers from commodity chemicals with favorable use properties. *J. Environ. Polymer Degrad.* **1995**, *3* (4), 215–223.
- Nimchua, T.; Punnapayak, H.; Zimmermann, W. Comparison of the hydrolysis of polyethylene terephthalate fibers by a hydrolyse from *Fusarium oxysporum* LCH I and *Fusarium solani* f. sp. pisi. *Biotechnol. J.* **2007**, *2*, 361–364.
- Figueroa, Y.; Hinks, D.; Montero, G. A heterogeneous kinetic model for the cutinase-catalyzed hydrolysis of cyclo-tris-ethylene terephthalate. *Biotechnol. Prog.* **2006**, *22* (4), 1209–1214.
- Ronkvist, A. M.; Wenhua, L.; Feder, D.; Gross, R. A. Cutinase catalyzed deacetylation of Poly(vinyl acetate). Manuscript in preparation.
- Karagiannidis, P. G.; Stergiou, A. C.; Karayannidis, G. P. Study of crystallinity and thermomechanical analysis of annealed poly(ethylene terephthalate) films. *Eur. Polym. J.* **2008**, *44*, 1475–1486.
- Pingping, Z.; Dezhui, M. Double cold crystallization peaks of Poly(ethylene terephthalate)- 1. Samples isothermally crystallized at low temperatur. *European Polym. J.* **1997**, *33* (10–12), 1817–1818.
- Xu, T.; Yuezhen, B.; Nakagaki, Y.; Matsuo, M. Density fluctuation of the amorphous region of Poly(ethylene terephthalate) films by quasi-spinodal decomposition. *Macromolecules* **2004**, *37*, 6985–6993.
- Lee, B.; Shin, T. J.; Lee, S. W.; Yoon, J.; Kim, J.; Ree, M. Secondary Crystallization behavior of Poly(ethylene isophthalate-co-terephthalate): Time-resolved small-angle X-ray Scattering and calorimetry studies. *Macromolecules* **2004**, *37*, 4174–4184.
- Melo, E. P.; Aires-Barros, M. R.; Costa, L.; Cabral, J. M. S. Thermal unfolding of proteins at high pH range studied by UV absorbance. *J. Biochem. Biophys. Methods* **1997**, *34*, 45–59.
- Petersen, S.; Fojan, P.; Petersen, E. I.; Neves Petersen, M. T. The thermal stability of the *Fusarium solani* pisi cutinase as a function of pH. *J. Biomed. Biotechnol.* **2001**, *1* (2), 62–69.
- Rodriguez, F.; Cohen, C.; Ober, C.; Archer, L. *Principles of Polymer Systems*, 5th ed.; Taylor & Francis: New York, 2003.
- Mochizuki, M.; Hiram, M.; Kanmuri, Y.; Kudo, K.; Tokiwa, Y. Hydrolysis of polycaprolactone fibers by lepace: Effect of draw ratio on enzymatic degradation. *J. Appl. Polym. Sci.* **1995**, *55*, 289–296.
- Abe, H.; Doi, Y. Structural effects on enzymatic degradabilities for Poly[(R)-3-hydroxybutyric acid] and its copolyesters. *Int. J. Biol. Macromol.* **1999**, *25*, 185–192.
- Yoo, E. S.; Im, S. S. Effect of crystalline and amorphous structures on biodegradability of Poly(tetra methylene Succinate). *J. Environ. Polym. Degrad.* **1999**, *7* (1), 19–26.
- Seretoudi, G.; Bikiaris, D.; Panayiotou, C. Synthesis characterization and biodegradability of poly(ethylene succinate)/poly(e-caprolactone) block copolymers. *Polymer* **2002**, *43*, 5405–5415.
- Timmins, M. R.; Lenz, R. W. Heterogeneous Kinetics of the Enzymatic Degradation of Poly(B-hydroxyalkanoates). *Polymer* **1997**, *38* (3), 551–562.
- Mukai, K.; Yamada, K.; Doi, Y., Kinetics and mechanism of heterogeneous hydrolysis of poly[(R)-3-hydroxybutyrate] film by PHA depolymerases. *Int. J. Biol. Macromol.* **1993**, *15* (December), 361–366.
- Kasuya, K.; Inoue, Y. Kinetics of Surface hydrolysis of poly[(R)-3-hydroxybutyrate] film by PHB depolymerase from *Alcaligenes faecalis* T1. *Polym. Degrad. Stab.* **1995**, *48*, 167–174.
- Scandola, M.; Focarete, M. L.; Frisoni, G. Simple kinetic model for the heterogenous enzymatic hydrolysis of natural Poly(3-hydroxybutyrate). *Macromolecules* **1998**, *31*, 3849–3851.
- Wu, C.; Jim, T. F.; Gan, Z.; Zhao, Y.; Wang, S. A heterogeneous catalytic kinetics for enzymatic biodegradation of poly(e-caprolactone) nanoparticles in aqueous solution. *Polymer* **2000**, *41*, 3593–3597.
- Herzog, K.; Mull, R. J.; Deckwer, W.-D. Mechanism and kinetics of the enzymatic hydrolysis of polyester nanoparticles by lipases. *Polymer Degrad. Stab.* **2006**, *91*, 2486–2498.
- Bailey, J. Enzyme kinetics of cellulose hydrolysis. *Biochem. J.* **1989**, *262*, 1001.
- Sattler, W.; Esterbauer, H. The effect of enzyme concentration on the rate of the hydrolysis of cellulose. *Biotechnol. Bioeng.* **1989**, *33*, 11221–1234.
- Nidetzky, B.; Zachariae, W.; Gercken, G.; Hayn, M.; Steiner, W. Hydrolysis of cellooligosaccharides by *Trichoderma reesei* cellohydrolases: Experimental data and kinetic modeling. *Enzyme Microb. Technol.* **1994**, *16*, 43–52.
- Canetti, M.; Urso, M.; Sadacco, P. Influence of the morphology and of the supermolecular structure on the enzymatic degradation of bacterial poly(3-hydroxybutyrate). *Polymer* **1999**, *40*, 2587–2594.